



Published in final edited form as:

*Genes Immun.* 2014 September ; 15(6): 392–403. doi:10.1038/gene.2014.30.

## The CLRX.1/NOD24 (NLRP2P) Pseudogene Codes a Functional Negative Regulator of NF- $\kappa$ B, Pyrin-only Protein 4 (POP4)

Kristen A. Porter<sup>1</sup>, Ellen B. Duffy<sup>1</sup>, Patricia Nyland<sup>1</sup>, Maninjay K. Atianand<sup>1,2</sup>, Hamayun J. Sharifi<sup>1</sup>, and Jonathan A. Harton<sup>1,\*</sup>

<sup>1</sup>Center for Immunology and Microbial Disease, Albany Medical College, 47 New Scotland Avenue, MC-151, Albany, NY 12208, USA

### Abstract

Pseudogenes are duplicated yet defunct copies of functional parent genes. However, some pseudogenes have gained or retained function. In this study we consider a functional role for the NLRP2-related, higher primate specific, processed pseudogene *NLRP2P*, which is closely related to Pyrin-only protein 2 (POP2/PYDC2), a regulator of NF- $\kappa$ B and the inflammasome. The *NLRP2P* open reading frame on chromosome X has features consistent with a processed pseudogene (retrotransposon), yet encodes a 45 amino acid, Pyrin-domain related protein. The open reading frame of *NLRP2P* shares 80% identity with POP2 and is under purifying selection across Old World primates. Although widely expressed, *NLRP2P* mRNA is upregulated by LPS in human monocytic cells. Functionally, *NLRP2P* impairs NF- $\kappa$ B p65 transactivation by reducing activating phosphorylation of RelA/p65. Reminiscent of POP2, *NLRP2P* reduces production of the NF- $\kappa$ B-dependent cytokines TNF $\alpha$  and IL-6 following TLR stimulation. In contrast to POP2, *NLRP2P* fails to inhibit the ASC-dependent NLRP3 inflammasome. In addition, beyond regulating cytokine production, *NLRP2P* has a potential role in cell cycle regulation and cell death. Collectively, our findings suggest that *NLRP2P* is a resurrected processed pseudogene that regulates NF- $\kappa$ B RelA/p65 activity and thus represents the newest member of the POP family, POP4.

### Keywords

Pyrin domain; pseudogene; NF- $\kappa$ B; NLR; inflammasome; inflammation

### Introduction

The innate immune system senses numerous danger and pathogen associated molecular patterns via germline-encoded pattern-recognition receptors (PRRs). These receptors include Toll-like receptors (TLRs), RIG-I helicase-like receptor, and NOD-like receptors (NLRs) (as reviewed in 1). Engagement of PRRs leads to cooperative signaling between MAPK and

\*Corresponding Author: 518-262-4445 (phone), 518-262-6161 (fax), hartonj@mail.amc.edu.

<sup>2</sup>Current address: Division of Infectious Diseases, University of Massachusetts Medical School, LRB, Rm 370M, 364 Plantation Street, Worcester, MA 01605

### Conflict of interest

The authors declare no conflict of interest.

NF- $\kappa$ B pathways to drive transcription of pro-inflammatory cytokines, assembly of NLR inflammasomes, and cell death.<sup>2</sup>

The nuclear factor- $\kappa$ B (NF- $\kappa$ B) family of transcription factors regulate expression of various cytokine genes involved in the immune response and inflammation, e.g. TNF $\alpha$ , IL-6 and IL-1 $\beta$  (as reviewed in 3). The NF- $\kappa$ B proteins RelA/p65, RelB, c-Rel, p50, p52 form homo- or heterodimers that control gene transcription.<sup>4</sup> NF- $\kappa$ B is generally sequestered in the cytoplasm by inhibitor of NF- $\kappa$ B (I $\kappa$ B) proteins. Upon stimulation, phosphorylation of I $\kappa$ B by IKK leads to I $\kappa$ B degradation, thus freeing the NF- $\kappa$ B dimer (p50/RelAp65, in the case of the canonical pathway), which translocates to the nucleus and drives transcription of target genes.<sup>3, 4</sup> Aberrant regulation of NF- $\kappa$ B results in a multitude of pathological conditions including multiple sclerosis, atherosclerosis, cancer, arthritis, Type I and Type II diabetes, and Alzheimer's disease.<sup>5</sup> Proper regulation of NF- $\kappa$ B is therefore highly desirable.

Mammalian genomes encode multiple NLR proteins,<sup>6</sup> PRRs which contain a central nucleotide-binding domain (NBD), C-terminal leucine rich repeats (LRR), and differing N-terminal 'effector' domains, typically a caspase recruitment domain (CARD) or pyrin domain (PYD).<sup>7</sup> CARD and PYD domains drive homodomain interactions facilitating the formation of an "inflammasome" complex by certain NLRs, thus recruiting and activating caspase-1 to cleave proIL-1 $\beta$  and proIL-18 to their active forms.<sup>8, 9</sup> Several human inflammatory and febrile diseases have been attributed to mutations within NLRP3<sup>10, 11</sup> and reviewed in 12, leading to the periodic or chronic overabundant IL-1 $\beta$  production responsible for the pathology. Moreover, given the role of IL-1 $\beta$  in innate inflammatory responses, polarization of Th17 cells,<sup>13-15</sup> and T-cell dependent antibody production,<sup>16, 17</sup> tight regulation of these inflammasome-dependent responses is important.

Interestingly, proteins capable of regulating NF- $\kappa$ B activation and inflammasome activation have recently emerged in higher primates,<sup>18, 19</sup> including the Pyrin-only proteins (POPs) which are composed strictly of a PYD.<sup>18, 20, 21</sup> Human POP1 and POP2 disrupt NF- $\kappa$ B at the level of IKK kinase activity and RelA/p65-mediated transactivation, respectively.<sup>18, 21, 22</sup> Further, POP2 disrupts the PYD:PYD interaction required for assembly and activity of some inflammasomes, including NLRP3.<sup>22</sup> However, POP3 regulates neither NF- $\kappa$ B nor NLRP3 inflammasomes, but instead inhibits formation of AIM2-like receptor (ALR) inflammasomes.<sup>20</sup> In mammals, POP genes are limited to hominids and Old World primates, suggesting an evolutionary pressure to control inflammatory response at both the level of cytokine gene transcription and processing of IL-1 $\beta$ .<sup>19, 22</sup> However, some viruses also encode POPs (vPOPs). Specifically, Myxoma protein (M013L) and Shope fibroma virus protein (SVF-gp013L) which are similar in sequence to POP1, inhibit PYD-dependent inflammasomes,<sup>23-25</sup> and impair NF- $\kappa$ B nuclear translocation.<sup>26</sup> In the case of myxoma virus, the M013L vPOP is required for virulence.<sup>24</sup>

Pseudogenes are defined as non-functional or defective copies of functional genes and classified as either processed or non-processed. Processed pseudogenes result from the retrotransposition of mRNA to a distal site in the genome without associated promoter or intron sequences.<sup>27</sup> Non-processed pseudogenes arise from gene duplication and typically

include both the proximal promoter elements and introns.<sup>28</sup> In both cases, premature stop codons, alternate splice sites, and other alterations generally prevent transcription and translation.<sup>29</sup> However, pseudogenes are not always indicative of non-functional sequences. The generation of pseudogenes may have been important for the development of variable region genes contributing to the diversity of immunoglobulins.<sup>30</sup> Further, transcribed processed pseudogenes, i.e. pseudogene mRNA, may play a role in regulating expression of their parent genes as is the case of pseudo-NOS<sup>31</sup> and PTENP1.<sup>32, 33</sup>

Two NLR pseudogenes, CLR12.1 and CLRX.1/NOD24 (NLRP2P), were previously identified in the human genome.<sup>7</sup> Of these, NLRP2P is interesting as both the POP2 and NLRP2P loci arose through retrotransposition of an *NLRP2/7*-like gene.<sup>19</sup> Notably, a syntenic NLRP2P locus is present in the genomes of humans, chimpanzees, orangutans, and Rhesus macaques.<sup>7, 19</sup> These loci each contain remnants of the NLRP2/7-like NBD and LRR coding domains as well as an ATG-initiated conserved open reading frame (ORF) comprising a short, but substantial, portion of the Pyrin domain. Therefore, we considered whether NLRP2P might represent a functional gene similar to POP2. Our data reveal that NLRP2 is expressed and inhibits NF- $\kappa$ B signaling upstream of pro-inflammatory cytokine release, albeit in a fashion somewhat different from POP2, suggesting that NLRP2P likely represents a resurrected pseudogene and a new member of the POP family.

## Results

### NLRP2P mRNA is expressed in human tissues

Retro-transposition of an *NLRP2/7*-like mRNA yielded a processed pseudogene which gave rise to a functional POP2 gene in Old World primates, apes, and humans.<sup>18, 19, 22</sup> Although *NLRP2P* was initially described as a pseudogene, the ORF codes for a predicted protein of 45 amino acids that shares with POP2 residues important for NF- $\kappa$ B inhibition. This warranted closer examination of the *NLRP2P* locus.

Pseudogenes result from either gene duplication followed by loss of expression and/or function (non-processed) due to random mutation events or by retro-transposition of an mRNA-derived sequence into a site distant from the parent locus that lacks the sequences needed for expression (processed). Table 1 compares the features of the *NLRP2P* locus with those of processed and non-processed pseudogenes. *NLRP2P* is located on chromosome X (distant from *NLRP2* and *NLRP7* on chromosome 19), contains a discernable poly-(A) tract near the remnants of the 3' end of the *NLRP2/7*-related sequence, lacks *NLRP2/7* introns, and has multiple stop codons. Therefore, *NLRP2P* most closely resembles a processed pseudogene. However, unlike true processed pseudogenes, *NLRP2P* retains an ORF largely corresponding to the first 45 codons of *NLRP2*. The human *NLRP2P* ORF sequence is 95, 91 and 92% homologous to *Pan troglodytes* (chimpanzee), *Pongo abelii* (orangutan) and *Macacca mulata* (rhesus macaque), respectively (*Pongo abelii*, has a stop codon after the first 19 codons, a mutation that likely occurred after the divergence of orangutans and chimps), suggesting sequence conservation expected to be absent in a pseudogene. Further, the *NLRP2P* record in the NCBI database (NG\_002752.4) predicts a short 68 bp intron downstream of the ORF that is absent in both *NLRP2* and *NLRP7*, a feature unexpected in DNA thought to be non-coding. Finally, multiple putative transcription factor binding sites

are present upstream of the ATG, suggesting a potential promoter region. These characteristics and the similarity of the translated *NLRP2P* ORF to *POP2* raised the possibility that *NLRP2P* might represent an expressed and potentially functional pseudogene.

To determine whether *NLRP2P* mRNA is transcribed, primers were designed to amplify a sequence downstream of the predicted stop codon, thus preventing detection of the highly similar *POP2* and *NLRP2* sequence (Fig. 1A). Further, based on sequence, *NLRP2P* primers were designed to span the predicted 68-bp intron, which was within the only unique sequence of the gene. Using these primers to screen a human cDNA tissue panel, we found that *NLRP2P* is expressed, at some level, in all tissues tested (Figure 1B). Weak expression was also detected in human endothelial cells (HUVEC), the macrophage cell line THP-1, and in primary human leukocytes.

Upon exposure to inflammatory stimuli (e.g. infection, LPS treatment), cells upregulate expression of various genes involved in mediating and regulating inflammation, including *POP2*.<sup>22</sup> Treatment of THP-1 cells with LPS increased expression of *NLRP2P* message (Fig. 1B), suggesting that *NLRP2P* may be induced during inflammation or infection. Interestingly, in poly(A)-purified cDNA tissue samples, the larger 220 bp amplicon corresponding to the non-spliced sequence was present in all samples, while the 153-bp amplicon, lacking the 68-bp intron, when detected, was weakly amplified and observed solely in the placenta, peripheral blood leukocytes, and bone marrow (Fig. 1B). Despite detection in all tissue types tested, *NLRP2P* was not detectable in epithelial (HeLa) or fibroblast-like (A293T) cells, suggesting that specialized cells within the respective tissue samples express *NLRP2P* and not the associated epithelium. Collectively, while *NLRP2P* has many characteristics similar of a processed pseudogene, these data demonstrate that *NLRP2P* produces an mRNA transcript in multiple human tissues, is induced by inflammatory stimuli, and may utilize a seemingly *de novo* intron in a tissue-restricted fashion. These processes are all inconsistent with the designation of *NLRP2P* as a pseudogene.

A physiological role is predicted for genes where non-synonymous mutations are selected against.<sup>34</sup> We recently demonstrated that *POP2* is under strong selective pressure and that the first 19 amino acids of *POP2* are necessary and sufficient for its function.<sup>19</sup> Therefore, we examined synonymous versus non-synonymous substitutions in *NLRP2P* between the human, chimp, and orangutan reference sequences as an indicator of evolutionary selective pressure (Fig. 2). The entire *NLRP2P* coding region appears to be under purifying selection regardless of which two species were compared (Fig. 2A–C). Codon-by-codon analysis using 2554 nt of sequence from each species also reveals purifying selection in the coding region with the exception of residues at positions 5, 21, 24, 27, 31, and 38 (Figure 2D). In the predicted human *NLRP2P* protein, all of these residues (except position 24) match *POP2*, suggesting a potential selective pressure toward the *POP2* sequence. Surprisingly, the in-frame sequence beyond the first stop codon in human and chimp *NLRP2P* ORF (codons 47–230) also appears to be under selection. Beyond codon 230 (codons 231–848), there is no evidence of selective pressure. Thus, like *POP2*, the retained coding sequence within *NLRP2P* is likely under recent and strong selective pressure, suggesting further that

*NLRP2P* is a functional gene. Collectively, these observations suggest that *NLRP2P* should no longer be considered a pseudogene, but rather a *bona fide* cellular gene, which we now term *POP4*.

### POP4 blocks NF- $\kappa$ B signaling at or downstream of RelA/p65

Given the above, POP4 is expected to be functionally comparable to POP2. The ORF of POP4 was therefore cloned into a FLAG-encoding expression vector. Since POP4 (45 a.a.) is shorter than POP2 (97 a.a.) and other Pyrin domains, POP4 likely forms only the first two  $\alpha$ -helices. The first  $\alpha$ -helix of POP2 is necessary and sufficient to inhibit transcription initiated by the transactivation domain 1 (TAD1) of NF- $\kappa$ B RelA/p65 (residues 519–540).<sup>22</sup> Further, the first  $\alpha$ -helix of POP4 is essentially identical to POP2 (Fig. 3A), differing only in residues shown to be dispensable for NF- $\kappa$ B inhibition.<sup>22</sup> Therefore, we anticipated that POP4 should inhibit NF- $\kappa$ B activation at or downstream of RelA/p65. Similar to POP1 and POP2, POP4 significantly reduced NF- $\kappa$ B promoter/reporter activity in response to TNF $\alpha$  (Fig. 3B). Expression of POP1 and POP2 in this system was confirmed by immunoblot (Fig. 3B, inset). Although the predicted molecular mass of POP4, approximately 5 kDa, likely accounts for our lack of detection by western blot, intracellular POP4 was detectable (Fig. 3B, right panel). Further, POP4, as well as POP2, reduced activation mediated by exogenously expressed RelA/p65 (Fig. 3C, left panel), but had no effect on transcription driven by the NF- $\kappa$ B independent SV40 promoter (Fig. 3C, right panel). As previously noted, POP1 does not impact the activity of RelA/p65. Together, these data suggest that, like POP2, POP4 acts at, or downstream of, RelA/p65 to block NF- $\kappa$ B activity.

### POP4 does not disrupt NLRP3 or ASC-mediated IL-1 $\beta$ release

PYD:ASC interactions are required for assembly of various inflammasomes critical to IL-1 $\beta$  release, including NLRP3 and AIM2.<sup>8, 35, 36</sup> POP2 disrupts ASC:PYD interactions<sup>18</sup> and blockade of inflammasome assembly by POP2 has been linked to  $\alpha$ -helices 1 and 4, however the first  $\alpha$  helix alone is necessary and sufficient to reduce inflammasome activity.<sup>22</sup> POP4 completely lacks PYD helices 4 through 6. In addition, POP4 lacks the acidic residues at positions 6 and 16 present in the first  $\alpha$  helix of POP2. Mutation of these residues in POP2 (E6Q and/or E16G) disrupts inhibition of the NLRP3 inflammasome.<sup>22</sup> Given the lack of helix 4 and non-acidic residues at positions 6 and 16 in POP4, we predicted that POP4 neither inhibits these inflammasomes nor impairs the release of mature IL-1 $\beta$ . Indeed, POP4 failed to prevent release of IL-1 $\beta$  from cells expressing a reconstituted NLRP3 inflammasome (Fig. 3D). Overexpression of ASC without an NLR in such reconstitutions also elaborates IL-1 $\beta$ , likely through either an endogenous unknown inflammasome scaffold protein or concentration-dependent oligomerization of ASC.<sup>22, 36, 37</sup> Regardless of mechanism, POP2 inhibits this inflammasome as well.<sup>22</sup> Even with increasing concentrations, POP4 was unable to block ASC-dependent IL-1 $\beta$  release (Fig. 3E). Therefore, POP4 appears not to be an inhibitor of the NLRP3 inflammasome and is unlikely to inhibit other ASC-dependent inflammasomes, suggesting a more exclusive role impacting the NF- $\kappa$ B signaling pathway.

## POP4 localizes to the nucleus upon TNF $\alpha$ stimulation, but does not alter RelA/p65 localization

In transfected HeLa cells, POP2 localizes primarily to the cytoplasm, but some cells demonstrate nuclear localization. Thus, we determined the cellular distribution of FLAG-tagged POP4 in HeLa cells. Although cytoplasmic localization was more predominant, some cells with nuclear concentration of POP4 were observed (Fig. 4A). POP2 may block p65 in part through reducing its nuclear presence,<sup>18</sup> and POP4 might function similarly. Therefore, we also examined the localization of POP4 and RelA/p65 following TNF $\alpha$  stimulation. Without treatment, localization of both POP4 and p65 was diffuse (Fig. 4B). However, by 30 minutes of TNF $\alpha$  stimulation, POP4 was predominately nuclear as was p65. Indeed, there was no significant difference in the number of cells displaying nuclear p65 following TNF $\alpha$  treatment in the presence or absence of POP4 (Fig. 4C), demonstrating that, surprisingly, unlike POP2, POP4 does not prevent or alter p65 nuclear localization. Further, TNF $\alpha$  treatment also induces the nuclear translocation of POP4 in the majority (80%) of transfected cells (Fig. 4D). The concomitant nuclear import of POP4 and p65 is consistent with our Gal4-p65 data and suggests that POP4 may limit p65 transcriptional activity in the nucleus.

## POP4 impairs p65 transactivation potential by reducing phosphorylation of S536

As POP4 blocks NF- $\kappa$ B p65 activity and POP2 is known to block p65 transactivation potential,<sup>22</sup> the ability of POP4 to disrupt p65 transactivation potential was determined. Cells were transfected with a construct producing the DNA-binding domain of Gal4 fused to the 30 amino acid, C-terminal transactivation domain 1 (TAD1) of p65 (residues 519–550), which drives transcription from a 5 $\times$ GAL4-luciferase reporter construct (Fig. 5A), and POP4 disruption of this activity was assessed. Similar to POP2, POP4 blocked transactivation by GAL4-p65 (TAD1), indicating that transactivation by the isolated TAD1 domain is inhibited (Fig. 5B). To further address the mechanism of NF- $\kappa$ B inhibition and explore the role of POP4 in macrophages, stable transfectants of POP4 were generated in the mouse J774A.1 cell line and three clones were isolated with various levels of POP4 expression (Fig. 5C, left panel). A polyclonal population of POP4 expressing J774A.1 cells was also produced by pooling POP4 expressing clones (Fig. 5C, right panel).

Phosphorylation of serine 536 (S536) within the TAD1 of p65 is essential for maximal transactivation in response to TNF $\alpha$  and LPS.<sup>4</sup> To determine whether POP4 impairs p65 transactivation by reducing S536 phosphorylation, p65 S536 phosphorylation status was monitored over time in nuclear and cytoplasmic fractions of the POP4-G7 cells post-TNF $\alpha$  treatment. At 5 minutes post-TNF $\alpha$ , phospho-S536 p65 (pp65) is detected in the nuclear fraction of the control transfectant (Fig. 5D). In contrast, the appearance of pp65 is largely attenuated in the POP4-G7 clone. The relative quantity of nuclear pp65 relative to total p65 was also determined for each time point (Fig. 5E). Based on this quantitation, after 5 minutes of TNF $\alpha$  treatment, nuclear pp65 accounts for approximately 90% of total p65, while by 30 minutes, nuclear pp65 in the POP4-G7 clone reaches only 40%. This suggests that POP4 is preventing the phosphorylation of RelA/p65 in J774A.1 cells. Nuclear accumulation of pp65 was measured for three independent clones (G7, D5 and B9) with graded POP4 expression (Fig. 5F). At the 5 minute time point, nuclear pp65 was reduced in

the B9, D5, and G7 clones to 30, 49 and 74%, respectively. The extent to which nuclear pp65 accumulation is diminished in these clones corresponds to their level of POP4 expression. Since nuclear accumulation of NF- $\kappa$ B is reflective of S536 phosphorylation status, we assessed the frequency of J774A.1 cells exhibiting nuclear p65 in POP4 clones D5 and G7 to further confirm that POP4 is reducing phosphorylation of p65 (Fig. 5G). As anticipated, both G5 and D7 POP4 clones exhibited fewer cells with nuclear pp65 at 10 and 30 minutes post-LPS treatment. Together these results strongly suggest that POP4 limits NF- $\kappa$ B phosphorylation of S536 in these cells, thereby reducing transactivation by the p65 TAD1. Curiously, although p65 translocation to the nucleus was largely unimpaired in HeLa cells, in J774-POP4 cells, nuclear fractions appear to contain less p65, however, nuclear translocation still occurs to a measurable degree. Nevertheless, POP4 reduces the amount of S536-phosphorylated p65 suggesting an impact of POP4 on a kinase or phosphatase targeting S536 and reducing the transactivation potential of RelA/p65. Given the inhibition of Gal4-p65 (TAD1), this is likely to occur in the nucleus.

The ability of RelA/p65 to protect cells from apoptotic death is well-studied using both RelA/p65 deficient mice, primary cells, and various transformed cell lines.<sup>38, 39</sup> Accordingly, the response to TNF $\alpha$ , (via RelA/p65) is important for development, immune homeostasis, and immune control of tumors.<sup>40</sup> Since POP4 inhibits RelA/p65, it may also influence cell survival. Inhibition of protein synthesis with cycloheximide (CHX) sensitizes HeLa cells to TNF $\alpha$  induced cytotoxicity.<sup>41</sup> POP4 expression in transfected HeLa cells did not significantly alter cellular proliferation with CHX and TNF $\alpha$  treatment, however in the presence of CHX alone, POP4 led to a reduction in cellular proliferation (Fig. 6A). Cell cycle analysis revealed that in CHX-treated cells POP4 disrupts progression through the S/G2 phase (Fig. 6B&C). Further, apoptosis (as indicated by hypodiploid nuclei) was significantly increased by POP4, but only in the presence of both CHX and TNF $\alpha$  (Fig. 6D). Surprisingly, under the same conditions, POP2, which also blocks p65 transactivation,<sup>22</sup> had no appreciable impact (Fig. 6D). These data suggest that under appropriate conditions POP4 might restrict cell cycle progression and promote apoptotic cell death, features consistent with its ability to inhibit RelA/p65.

### **POP4 reduces pro-inflammatory cytokine release elicited by TLR ligands or infection**

In macrophages, POP4 reduction in p65 transactivation is predicted to reduce NF- $\kappa$ B-dependent cytokine elaboration. We therefore monitored the impact of POP4 expression on production of the NF- $\kappa$ B-dependent cytokines TNF $\alpha$  and IL-6 following stimulation with the TLR1/2 agonist Pam3CysK4 and the TLR4 agonist LPS. TLR2 agonists are weak inducers of IL-6 in both cell lines and primary murine macrophages, whereas TLR4 agonists are strong inducers.<sup>42</sup> We obtained similar results following Pam3CysK4 and LPS stimulation of J774A.1 macrophages, where Pam3CysK4 induced picogram quantities of IL-6 versus the nanogram quantities seen with LPS (Fig. 7A&B). However, in both individual and polyclonal populations of stable-transfected POP4-expressing J774A.1 cells, POP4 reduced IL-6 and TNF $\alpha$  release relative to vector-only controls in response to LPS (Fig. 7A) and Pam3CysK4 (Fig. 7B). Additionally, TNF $\alpha$  was also reduced in POP4-expressing J774 cells compared to controls following infection with the mouse pathogen *Francisella tularensis ssp. novicida* (U112, Fig. 7C),<sup>43</sup> which is recognized by TLR2.<sup>44</sup>

These gain-of-function studies demonstrate that production of the NF- $\kappa$ B-dependent cytokines TNF $\alpha$  and IL-6 following stimulation with different PAMPs is reduced by POP4 and suggest that *in vivo*, POP4 may act to regulate human macrophage production of NF- $\kappa$ B-dependent, pro-inflammatory cytokines.

To confirm a likely physiological role for POP4 in human myeloid cells, we attempted an RNAi knockdown of POP4 in PMA-differentiated THP-1 cells and examined the production of IL-6 and TNF $\alpha$ . A unique sequence in the 3'UTR of POP4 (Fig. 1A) was targeted using siRNA. Not surprisingly, since RNA is a TLR3 agonist and TLR4 engagement lead to POP4 expression, POP4 message was similarly induced following transfection with any RNA duplex, PMA, or LPS (Fig. 7D). Therefore, we utilized varying concentrations of POP4 siRNA to determine at what dose POP4 knockdown could be achieved. In contrast to THP-1 cells treated with LPS alone, knockdown of POP4 expression was observed in LPS treated THP-1 receiving 250 ng of POP4 siRNA (~1.0 pg/cell) (Fig 7D). Introduction of greater quantities of POP4 siRNA were less effective, likely due to the competing ability of the RNA duplexes to induce additional POP4 expression. In cells with reduced POP4 expression (250 ng siRNA), there was a statistically significant increase in IL-6 and TNF $\alpha$  cytokine release as compared to control cells (Fig. 7E). Cells exhibiting induction of POP4 relative to controls produced slightly reduced levels of IL-6 and TNF $\alpha$  (data not shown). Thus the relative absence of POP4 is associated with increased TNF $\alpha$  and IL-6 production, demonstrating that the impact of POP4 on NF- $\kappa$ B-dependent cytokine production in mouse macrophages can be extended to cells of human origin. These results are highly similar to those previously obtained with POP2,<sup>22</sup> consistent with the high degree of sequence similarity between these proteins.

## Discussion

Collectively, our findings support the re-classification of the higher primate-restricted NLRP2P pseudogene (CLR.X.1/NOD24) as a functional gene, pyrin-only protein 3 (POP4). Initially thought to be inert, POP4 exhibits the capacity to negatively regulate NF- $\kappa$ B p65 activity through reduction of S536 phosphorylation within the TAD 1 of p65. This mechanism likely accounts for the reduced production of NF- $\kappa$ B-dependent proinflammatory cytokines downstream of TLR signals when POP4 is expressed.

During the course of higher primate evolution, an *NLRP2*-like message gave rise to two apparent pseudogenes now evident within the human genome. One of these pseudogenes, *POP2*, was whittled down from the much larger *NLRP2*-like sequence into a single exon gene, gained a promoter, developed a 3'UTR, and has recently been appreciated for both its ability to reduce NF- $\kappa$ B signaling and disrupt the NLRP3 inflammasome,<sup>18, 19, 22</sup> features consistent with a newly emergent gene. Until this study, nothing was known about the other pseudogene, *NLRP2P/POP4* beyond its presence in the genome. Although a non-coding *POP2* processed pseudogene is present in the marmoset genome, no sequence data is available at present for the syntenic portion of marmoset chromosome X corresponding to *NLRP2P*. No sequences orthologous to *POP4* were detected in the available New World primate genomes. Thus, it is presently unknown whether the insertion event leading to the *NLRP2P* locus occurred prior to, or after, the divergence of Old and New World primate



species. Further, in all species examined, *POP4* retains the non-coding remnants of the still discernable *NLRP2*-like sequences. Given the expression of *POP4*, its function, and the apparent lack of more refined 5' and 3' UTRs, *POP4* appears to be a gene in the midst of emerging from a processed pseudogene to a functional gene. The appearance of both *POP2* and *POP4* in higher primates demonstrates recent and strong selective pressure acting within these species. Although the nature of this selective pressure is unknown, a deleterious impact on the signaling pathways associated with innate immunity and inflammation which POPs counteract is likely.

Over time, *POP4* gained a unique insertion, a 68-bp intron within its 3'UTR which is occasionally spliced in mRNA from peripheral blood leukocytes, bone marrow, and most dramatically in the placenta. While this insertion could simply be the whittling away of non-coding *NLRP2* remnants, these splice variants could serve a function. For example, the presence or absence of the intron may alter message expression, as observed for the tissue-specific element in the first intron of *N-myc*.<sup>45</sup> Such a process could effectively restrict POP4 protein expression to those cells with the appropriate splice variant. Another possibility is that POP4 message may regulate itself or another related transcript (i.e. *POP2* or *NLRP2*). Such gene targeted regulation has been described for some transcribed processed pseudogenes including control of neural nitric oxide synthase (nNOS) by its pseudogene, *pseudo-NOS*<sup>31</sup> and PTEN by its pseudogene, *PTENP1*.<sup>32, 33</sup> However, the observation that a cDNA version of *POP4* exhibits the same function reflected by siRNA knockdown and that this function is consistent with our mutational studies of the POP2 protein support that POP4 is most likely acting as a protein.

Unlike POP2, neither POP4 nor POP1 block IL-1 $\beta$  release from the NLRP3 inflammasome in reconstitution assays. While POP1 differs sufficiently from POP2 and POP4 to account for the observed lack of inflammasome inhibition, POP4 maintains a first  $\alpha$ -helix almost identical to that of POP2. The inability of POP4 to block inflammasomes initiated by NLRP3 or ASC overexpression together with the absence of negatively charged residues at positions 6 and 16 that are critical for inhibition of these inflammasomes by POP2,<sup>22</sup> further establishes the importance of these residues for this function of POP2. Still, that POP4 might interfere with other inflammasomes remains possible.

Our work also highlights the dynamics of NF- $\kappa$ B activity and complexity in its cellular localization. As the physiological baseline levels, activation pathways, post-translational modifications, repressors, and outcomes differ between cell type and stimulus, NF- $\kappa$ B signaling is considered so complicated that the use of an "NF- $\kappa$ B pathway interactome" model has been proposed in place of the canonical pathway-centric model to study NF- $\kappa$ B.<sup>46</sup> POP4 effectively inhibits NF- $\kappa$ B at the level of p65, apparently through reducing S536 phosphorylation. How this is accomplished is unclear. Although we have not detected any physical interaction between p65 and POP2 or POP4, several kinases target S536, including IKK $\alpha$ . POP1 is reported to inhibit cytosolic IKK $\alpha$  and  $\beta$  upstream of I $\kappa$ B $\alpha$  phosphorylation, thus preventing nuclear translocation of p50:p65 heterodimers in epithelial cells.<sup>21</sup> However, since POP4 does not inhibit the localization of p65 in HeLa cells, it is more likely that POP4 prevents the action of another S536 kinase. A more extensive time course of p65-S536 phosphorylation and consideration of whether the targeted phosphorylation event occurs

prior to or after nuclear localization may be revealing and may help account for differences in p65 nuclear localization observed between mouse and human cell lines when POP4 is present. Alternatively we cannot rule out the possibility that POP4 activates a phosphatase active towards NF- $\kappa$ B p65. Whether POP4 might also inhibit TAD2 activity or DNA binding by NF- $\kappa$ B is not yet known.

Like POP2, POP4 is induced by inflammatory stimuli consistent with its likely role as regulator of inflammatory cytokine production. Curiously, exposure of THP-1 cells to siRNA duplexes leads to POP4 expression, suggesting that engagement of RNA sensing receptors (e.g. TLR3 or RLRs) may drive POP4 expression in an IRF3-dependent fashion. Whether TLR3 or IRF3 are necessary for POP4 induction will be the subject of further investigation. The impact of POP4 siRNA knockdown in THP-1 cells and heterologous expression of POP4 in J774A.1 cells on the production of LPS-induced TNF $\alpha$  is comparable to that seen with POP2 in similar experiments.<sup>22</sup> However, POP4 has a more profound effect upon Pam-3CysK-induced TNF $\alpha$ , than previously observed for POP2. While these comparisons may reflect technical variations, it remains possible that POP4 acts more extensively than POP2 or has an additional capacity to influence TLR2 signals leading to TNF $\alpha$ . Collectively, the action of POP4 to temper inflammatory cytokine responses is very similar to that seen with POP2 and supports the hypothesis that POPs serve as a family of inflammatory regulators.

Beyond its impact upon the inflammatory response elicited by macrophages, POP4 appears to promote cell cycle arrest at S/G2/M and contribute to apoptotic cell death in HeLa cells. Although likely a consequence of RelA/p65 inhibition by POP4, these studies do not rule out other potential explanations. In fact, the inability of POP2, which also inhibits NF- $\kappa$ B, to mediate similar effects suggests an unexpected function that may be distinct from NF- $\kappa$ B inhibition or reflect unappreciated differences in the magnitude or mechanism of inhibition. It will be of interest to further consider the role of POP2 and POP4 in cell cycle control and survival. Nevertheless, the results of these experiments are important as a role beyond controlling inflammation is implicated. Specifically, since POP4 is broadly expressed and demonstrates enhancement of apoptotic activity in a transformed cell line, it may have a role in tumor suppression.

Again, this initial characterization of POP4 has the potential to reveal aspects of POP2 function. POP4 is approximately half the size of POP2 (due to the stop codon which precludes translation of  $\alpha$ -helices 4–6) and lacks key amino acids in  $\alpha$ 1 and  $\alpha$ 2 that are important for inflammasome inhibition by POP2. The first  $\alpha$ -helix of POP2 in isolation is sufficient to disrupt p65 activity,<sup>22</sup> consistent with our POP4 data. However, localization of p65 is clearly not altered by POP4 in HeLa cells, unlike POP2 which appears to have multiple impacts on p65 localization including both blockade of nuclear import, nuclear redistribution, and generalized loss of p65.<sup>18</sup> Further, POP4 translocates to the nucleus upon TNF $\alpha$  stimulation, which is not observed for full-length POP2.<sup>18</sup> These observations suggest that the later helices of POP2, absent in POP4, might account for the different pattern of POP2 localization, the loss of nuclear p65 in POP2 expressing cells following TNF $\alpha$  stimulation and its inability to promote apoptosis and cell growth defects.

We have demonstrated that a previously classified pseudogene, *NLRP2P*, encodes a functional gene product (POP4) similar to POP2 in sequence and the capacity to regulate NF- $\kappa$ B-dependent pro-inflammatory responses. Considering its function and its sequence relation to POP2, should POP4 be considered a pyrin-only protein? As members of the death domain fold superfamily, PYDs have five to six amphipathic  $\alpha$ -helices.<sup>47</sup> The 45 a.a. of POP4 code for only two of these, yet this study and our work with POP2 demonstrate the functional importance of this region. Thus it seems reasonable to include variants of the pyrin domain as members of the POP family. Finally, the very small size of POP4 raises the possibility that other small, but potentially overlooked genes remain to be discovered, a likelihood highlighted by the paucity of studies examining the roles of a similarly sized family of CARD-only proteins (COPs) thought to prevent caspase-1 recruitment to the inflammasome.<sup>48</sup>

Why do higher primates have multiple POPs? Are POPs redundant? While POP1, POP2, and POP4 have seemingly overlapping functions, they operate at different points (and in potentially different locales) during NF- $\kappa$ B activation. Most recently, POP3, a regulator of the ALR inflammasome formed by AIM2, was described<sup>20</sup>. Whether POP3 regulates the NF- $\kappa$ B pathway in any fashion remains unknown at this time. POP1 acts upstream of NF- $\kappa$ B release at the level of IKK, but, like POP4, without inhibiting the inflammasome. POP2 inhibits the inflammasome, but also inhibits NF- $\kappa$ B downstream at p65 transactivation, like POP4. However, POP4 localization may be predominantly nuclear following stimulation, unlike the infrequently nuclear POP2. Additionally, POP4 expression appears ubiquitous in human tissues in contrast to POP2 which displays constitutive expression restricted to testis and PBLs. This suggests non-redundancy and the possibility of cooperative regulation of inflammatory signals where three POPs with different modalities may modulate inflammatory responses at multiple steps within the pathway; from stimuli to signaling, to gene transcription, cytokine processing and eventually homeostasis. Verification of this hypothesis would establish that primate species possessing POPs have developed a complex system for regulating the response pathways leading to inflammation which is likely important for our understanding of acute and chronic inflammation in human health and disease.

## Materials and Methods

### Cell lines

J774A.1, HEK-293, HEK-293T and THP-1, A293T and HeLa cell cultures and maintenance have been previously described.<sup>18, 22</sup> HUVECs (graciously provided by Dr. Mohamed Treback, Albany Medical College) were maintained in EMG-2 media (Lonza, Walkersville, MD, USA).

### RNA extraction and RT-PCR

Cytoplasmic RNA from cell lines was extracted using the RNeasy Kit (Qiagen, Valencia, CA, USA) and treated with DNase (Qiagen) to eliminate chromosomal DNA contamination. DNA-free RNA (500 ng) was reverse transcribed and amplified using the

OneStep RT-PCR Kit (Qiagen) as directed by the manufacturer with the primers described below.

### POP4 expression studies

cDNA (5 ng) from the Human MTC™ Panel I and Human Immune System MTC™ Panel (Clontech, Mountainview, CA, USA) was used to detect POP4 expression in human tissues. Primers (Forward: 5'-GCGTTTCGAAGCAGAAGCACTAGA-3', Reverse: 5'-GCTGAACGGGATCAGCATCTTGTA-3') were designed to specifically amplify within the NLRP2P 3'UTR (Genbank Accession No.BK001116.1), a region which lacks homology with POP2 and NLRP2. GAPDH primers have been described previously.<sup>49</sup> For expression in human non-hemopoietic cell lines, RNA was extracted from approximately  $1 \times 10^6$  untreated cells. THP-1 cells were cultured with or without LPS (100 ng/mL) 24 h prior to RNA extraction. Amplification conditions were as follows: 94°C for 5 min, 35 cycles of 94°C-30 s, 55°C-15 s, 72°C-30 s.

### Sequence analysis

One dimensional sliding window analysis of Ka and Ks (SWAKK) analysis was performed using the SWAKK algorithm ([oxytricha.princeton.edu/SWAKK](http://oxytricha.princeton.edu/SWAKK)) with a window of 30. Codon comparisons were performed using the Muse-Gaut model<sup>50</sup> of codon substitution and Tamura-Nei model<sup>51</sup> of nucleotide substitution to produce a joint Maximum Likelihood reconstructions of ancestral states and a tree. The test statistic  $dN - dS$  is used for detecting codons that have undergone positive selection, where  $dS$  is the number of synonymous substitutions per site ( $s/S$ ) and  $dN$  is the number of nonsynonymous substitutions per site ( $n/N$ ). A positive value for the test statistic indicates an overabundance of nonsynonymous substitutions. In this case, the probability of rejecting the null hypothesis of neutral evolution (P-value) is calculated and values of P less than 0.05 are considered significant.<sup>52, 53</sup> Normalized  $dN - dS$  for the test statistic is obtained using the total number of substitutions in the tree (measured in expected substitutions per site). Maximum Likelihood computations of  $dN$  and  $dS$  were conducted using HyPhy software package.<sup>54</sup> The analysis included nucleotide sequences for the NLRP2P locus from human, chimpanzee, and orangutan. All positions containing gaps and missing data were eliminated. There were a total of 848 positions in the final dataset. Evolutionary analyses were conducted using the MEGA5 software package.<sup>55</sup>

### siRNA

Control and siRNA duplexes are as follows: 5' ACG AGG AGA UGU CAC GAC CCG AUA A 3' and 5' CUU CUC UUA GGC UGG UGA CAU CUU CCU 3', respectively. THP-1 cells were seeded at  $2.5 \times 10^5$  and treated with 100 nM PMA. Cells were transfected 24 h later with indicated concentrations of duplex at a 3:1 ratio of FuGene 6 (Roche Applied Science, Indianapolis, IN, USA). Cells were treated 18h post-transfection with 200 ng/mL LPS and 6 h later, RNA was extracted from cells and used for RT-PCR, and cytokines in the supernatants were analyzed by cytometric bead array (Bio-Rad, Hercules, CA, USA).

## POP4 cloning

The coding sequence from the ATG start site to the first stop codon of POP4 was synthesized and cloned into the pIDTSMART-AMP vector by IDT, Inc. (Coralville, IA, USA). Using added EcoRI and XhoI sites, POP4 was then cloned in-frame into pcDNA3-FLAG and pcDNA3-myc to produce FLAG- and Myc-tagged forms respectively. The cloned POP4 sequence was confirmed by sequencing.

## Generation of J774A.1 stable transfectants

Stable POP4 and control transfectants were produced as previously described.<sup>22</sup> Briefly,  $5 \times 10^6$  J774A.1 cells were electroporated with 10  $\mu$ g of PvuI linearized FLAG-POP4 or vector-only DNA (570V, 25 $\mu$ F) followed by selection in G418 (1 mg/mL) and isolation of clonal populations.

## Flow cytometry

POP4 expression was confirmed in transiently transfected HEK-293T or stable J774 clones by immunolabeling the FLAG tag followed by flow cytometry. HEK-293T cells were fixed in 1% paraformaldehyde for 30 min, permeabilized with saponin (30 min), followed by blocking with 1% BSA. J774 clones ( $10^6$  cells) were incubated with 0.5  $\mu$ g of rat anti-mouse CD16/CD32 (Mouse BD Fc Block, BD Biosciences, San Jose, CA, USA) for 15 min on ice to block Fc receptors and then permeabilized and fixed using Cytotfix/Cytoperm Plus (BD Biosciences), according to manufacturer's instructions. Cells were stained with (1:500) anti-FLAG M2 (Sigma-Aldrich, St. Louis, MO, USA) for 45 min on ice followed by (1:2000) goat anti-mouse Alexafluor 647 (Abcam, Cambridge, MA, USA) (HEK-293T) or (1:500) goat anti-mouse Alexafluor 488 (Invitrogen, Camarillo, CA, USA) (J774) for 30 min. Mouse IgG1 (1:2000) was used as for isotype control staining. Fluorescence staining was assayed using a FACSCanto flow cytometer (BD Biosciences) and the resulting data was analyzed using FlowJo 7.2.2 software (Tree Star, Ashland, OR, USA). Clonal populations (clones G7, D5, and B9) were selected for experiments based on the range of FLAG expression levels. For cytokine induction experiments a polyclonal population (Poly) comprised of several POP4-expressing clones was used to rule out clonal effects.

## Cell proliferation and nuclei analysis

For proliferation, HeLa cells were seeded at  $5 \times 10^4$  and transfected the next day with empty vector (EV) or POP4 constructs, and then either left untreated or treated with cycloheximide (20  $\mu$ g/mL, CHX), TNF $\alpha$  (5 ng/mL), or CHX and TNF $\alpha$  for 24 h. Cells were then counted via trypan blue and the cell growth was determined. For PI staining, HeLa cells were seeded at  $1.5 \times 10^5$  and the next afternoon transfected with empty vector (EV), POP2 or POP4 constructs and pLaminB-GFP<sup>56</sup>, and 24 h later cells were either left untreated or treated with TNF $\alpha$  (5 ng/mL) and/or CHX (20  $\mu$ g/mL). Flow cytometry and PI analysis of GFP+ nuclei (suggestive of transfected cells) was done as previously described.<sup>56</sup> Nuclei and cell cycle values were determined using FlowJo 7.2.2 software.

## NF- $\kappa$ B luciferase and inflammasome reconstitution assays

NF- $\kappa$ B luciferase assays were performed as described previously.<sup>18</sup> Briefly, HEK-293 cells were transfected with 3 $\times$ NF- $\kappa$ B luciferase reporter (100 ng) and 24 h later treated with TNF $\alpha$  (10 – 20 ng/mL) to induce endogenous NF- $\kappa$ B. Following another 24 h, cells were lysed and luciferase activity quantified. Alternatively, 293T cells were cotransfected with either an empty vector or a POP expression vector (1  $\mu$ g) and p65 (100 ng), and 24 h post transfection cells were lysed and luciferase activity quantified. HEK293T cells were used to reconstitute the inflammasome as described previously.<sup>22</sup> Cells were seeded at  $5 \times 10^4$  cells well<sup>-1</sup> in 24-well plates. Following overnight culture, the cells were transfected with plasmids encoding pro-caspase-1 (50 ng), pro-IL-1 $\beta$  (200 ng), ASC (10 ng), and NLRP3 (100 ng) in the absence or presence of POPs (500 ng). For determination of the dose response to POP4, 293T cells were transfected with plasmids encoding pro-caspase 1 and pro-IL-1 $\beta$  as indicated above, ASC (400 ng) and POP4 (0 ng to 1000 ng). Approximately 20 h post-transfection, culture supernatants were harvested, centrifuged briefly to remove cellular debris, and used for the measurement of secreted IL-1 $\beta$  by ELISA (Invitrogen).

## Immunofluorescence and western blotting

HeLa cells, transfected with 1  $\mu$ g of FLAG-POP4 or vector, were left untreated or treated for 30 min with TNF $\alpha$  (20 ng/mL) and stained as previously described using anti-FLAG M2.<sup>18</sup> Images were obtained using a Zeiss Axio Observer.Z1 fluorescence microscope. To determine the fraction of POP4 expressing cells demonstrating nuclear localization of p65, POP4 positive cells (>100) were counted and the percentage with nuclear p65 staining was expressed as a percentage of all cells counted. For western blotting,  $1 \times 10^5$  J774 cells were seeded and the next day treated with mTNF $\alpha$  (20 ng/mL). Nuclear and cytoplasmic proteins were fractionated using NE-PER Nuclear and Cytoplasmic Extraction Reagents (Thermo Sci., Rockford, IL, USA). Antibodies used were Rb pS536-p65 (1:1000), Rb anti-p65 (1:500), and Rb  $\beta$ -actin (1:1000). All antibodies were from Cell Signaling Tech (Danvers, MA, USA). Secondary antibody goat anti-rabbit-HRP was from Santa Cruz Biotech (Santa Cruz, CA, USA) at 1:5000. SuperSignal West Dura Substrate (Thermo Sci.) was used and chemiluminescence was detected on film. Densitometric analysis was performed using ImageJ software (U. S. National Institutes of Health, Bethesda, MD, USA).

## Immunofluorescence detection of nuclear p65

J774A.1 clones stably expressing POP4 were seeded at  $3 \times 10^6$  in 60mm dishes and allowed to adhere prior to treatment with 200 ng/ml LPS (O26:B6; Sigma-Aldrich). Cells were fixed in 1% PFA (30 min), permeabilized with saponin (30 min) and stained with (1:50) anti p65-NF- $\kappa$ B (Santa Cruz Biotech, Santa Cruz, CA, USA) for 20 min followed by (1:200) goat anti-rabbit Alexafluor 488. Cells were washed with PBS containing 2% FBS and 1mM EDTA to prevent clumping and stored in 1% PFA at 4C. Nuclei were stained with (1:5000) DRAQ5 (Cell Signaling Technology, Danvers, MA, USA) for 5 min prior to analysis. Cells were analyzed on an ImageStream<sup>X</sup> MKII Fluorescence Cytometer (Amnis, Seattle, WA, USA) and images acquired and processed using the Image Stream Data Exploration and Analysis software (IDEAS). Percent nuclear p65 was calculated using a similarity analysis with a score of 2 or higher indicating nuclear NF- $\kappa$ B distribution<sup>57</sup>.

## Statistics

Unless otherwise indicated, data shown is the mean of at least three independent experiments and error bars indicate SEM. Student's *t* test (two-sample, unequal variance) was used to calculate *p* values.

## Acknowledgements

The authors thank Dr. James R. Drake for critical review of this manuscript, Dr. Carlos M. de Noronha for reagents, Amithi Narendran for technical support, and the AMC Immunology Core. This work was supported by National Research Service Award (1F32AI100473-01) to KAP and National Institutes of Health grant (R01AI072259) awarded to JAH.

## References

1. Martinon F, Mayor A, Tschopp J. The inflammasomes: guardians of the body. *Annu Rev Immunol.* 2009; 27:229–265. [PubMed: 19302040]
2. Meylan E, Tschopp J, Karin M. Intracellular pattern recognition receptors in the host response. *Nature.* 2006; 442:39–44. [PubMed: 16823444]
3. Ghosh S, Hayden MS. New regulators of NF- $\kappa$ B in inflammation. *Nat Rev Immunol.* 2008; 8:837–848. [PubMed: 18927578]
4. Huang B, Yang X-D, Lamb A, Chen L-F. Posttranslational modifications of NF- $\kappa$ B: Another layer of regulation for NF- $\kappa$ B signaling pathway. *Cellular Signal.* 2010; 22:1282–1290.
5. Hayden MS, Ghosh S. NF- $\kappa$ B, the first quarter-century: remarkable progress and outstanding questions. *Genes Dev.* 2012; 26:203–234. [PubMed: 22302935]
6. Saleh M. The machinery of Nod-like receptors: refining the paths to immunity and cell death. *Immunol Rev.* 2011; 243:235–246. [PubMed: 21884180]
7. Harton JA, Linhoff MW, Zhang J, Ting JPY. Cutting Edge: CATERPILLER: A Large Family of Mammalian Genes Containing CARD, Pyrin, Nucleotide-Binding, and Leucine-Rich Repeat Domains. *J Immunol.* 2002; 169:4088–4093. [PubMed: 12370334]
8. Martinon F, Burns K, Tschopp J. The inflammasome: a molecular platform triggering activation of inflammatory caspases and processing of proIL- $\beta$ . *Mol Cell.* 2002; 10:417–426. [PubMed: 12191486]
9. Kayagaki N, Warming S, Lamkanfi M, Walle LV, Louie S, Dong J, et al. Non-canonical inflammasome activation targets caspase-11. *Nature.* 2011; 479:117–121. [PubMed: 22002608]
10. Brydges SD, Mueller JL, McGeough MD, Pena CA, Misaghi A, Gandhi C, et al. Inflammasome-Mediated Disease Animal Models Reveal Roles for Innate but Not Adaptive Immunity. *Immunity.* 2009; 30:875–887. [PubMed: 19501000]
11. Agostini L, Martinon F, Burns K, McDermott MF, Hawkins PN, Tschopp J. NALP3 Forms an IL-1 $\beta$ -Processing Inflammasome with Increased Activity in Muckle-Wells Autoinflammatory Disorder. *Immunity.* 2004; 20:319–325. [PubMed: 15030775]
12. Mitroulis I, Skendros P, Ritis K. Targeting IL-1 $\beta$  in disease; the expanding role of NLRP3 inflammasome. *Eur J Int Med.* 2010; 21:157–163.
13. Dunne A, Ross PJ, Pospisilova E, Masin J, Meaney A, Sutton CE, et al. Inflammasome Activation by Adenylate Cyclase Toxin Directs Th17 Responses and Protection against *Bordetella pertussis*. *J Immunol.* 2010; 185:1711–1719. [PubMed: 20610650]
14. Gris D, Ye Z, Iocca HA, Wen H, Craven RR, Gris P, et al. NLRP3 Plays a Critical Role in the Development of Experimental Autoimmune Encephalomyelitis by Mediating Th1 and Th17 Responses. *J Immunol.* 2010; 185:974–981. [PubMed: 20574004]
15. Chung Y, Chang SH, Martinez GJ, Yang XO, Nurieva R, Kang HS, et al. Critical Regulation of Early Th17 Cell Differentiation by Interleukin-1 Signaling. *Immunity.* 2009; 30:576–587. [PubMed: 19362022]

16. Nakae S, Asano M, Horai R, Sakaguchi N, Iwakura Y. IL-1 Enhances T Cell-Dependent Antibody Production Through Induction of CD40 Ligand and OX40 on T Cells. *J Immunol.* 2001; 167:90–97. [PubMed: 11418636]
17. Nakae S, Asano M, Horai R, Iwakura Y. Interleukin-1 $\beta$ , but not interleukin-1 $\alpha$ , is required for T-cell-dependent antibody production. *Immunology.* 2001; 104:402–409. [PubMed: 11899425]
18. Bedoya F, Sandler LL, Harton JA. Pypin-only protein 2 modulates NF-kappaB and disrupts ASC:CLR interactions. *J Immunol.* 2007; 178:3837–3845. [PubMed: 17339483]
19. Atianand MK, Fuchs T, Harton JA. Recent evolution of the NF-kappaB and inflammasome regulating protein POP2 in primates. *BMC Evol Biol.* 2011; 11:56. [PubMed: 21362197]
20. Khare S, Ratsimandresy RA, de Almeida L, Cuda CM, Rellick SL, Misharin AV, et al. The PYRIN domain-only protein POP3 inhibits ALR inflammasomes and regulates responses to infection with DNA viruses. *Nat Immunol.* 2014; 15:343–353. [PubMed: 24531343]
21. Stehlik C, Krajewska M, Welsh K, Krajewski S, Godzik A, Reed JC. The PAAD/PYRIN-only protein POP1/ASC2 is a modulator of ASC-mediated nuclear-factor-kappa B and pro-caspase-1 regulation. *Biochem J.* 2003; 373:101–113. [PubMed: 12656673]
22. Atianand MK, Harton JA. Uncoupling of Pypin-only protein 2 (POP2) mediated dual-regulation of NF- $\kappa$ B and the inflammasome. *J Biol Chem.* 2011
23. Dorfleutner A, Talbott SJ, Bryan NB, Funya KN, Rellick SL, Reed JC, et al. A Shope Fibroma virus PYRIN-only protein modulates the host immune response. *Virus Genes.* 2007; 35:685–694. [PubMed: 17676277]
24. Johnston JB, Barrett JW, Nazarian SH, Goodwin M, Ricuttio D, Wang G, et al. A Poxvirus-Encoded Pypin Domain Protein Interacts with ASC-1 to Inhibit Host Inflammatory and Apoptotic Responses to Infection. *Immunity.* 2005; 23:587–598. [PubMed: 16356857]
25. Rahman MM, McFadden G. Myxoma Virus Lacking the Pypin-Like Protein M013 Is Sensed in Human Myeloid Cells by both NLRP3 and Multiple Toll-Like Receptors, Which Independently Activate the Inflammasome and NF- $\kappa$ B Innate Response Pathways. *J Virol.* 2011; 85:12505–12517. [PubMed: 21957307]
26. Rahman MM, Mohamed MR, Kim M, Smallwood S, McFadden G. Co-regulation of NF-kappaB and inflammasome-mediated inflammatory responses by myxoma virus pypin domain-containing protein M013. *PLoS Pathog.* 2009; 5:e1000635. [PubMed: 19851467]
27. Khurana E, Lam HY, Cheng C, Carriero N, Cayting P, Gerstein MB. Segmental duplications in the human genome reveal details of pseudogene formation. *Nucleic Acids Res.* 2010
28. Sen K, Podder S, Ghosh TC. Insights into the genomic features and evolutionary impact of the genes configuring duplicated pseudogenes in human. *Febs Letters.* 2010; 584:4015–4018. [PubMed: 20708614]
29. D'Errico I, Gadaleta G, Saccone C. Pseudogenes in metazoa: origin and features. *Brief Funct Genomic Proteomic.* 2004; 3:157–167. [PubMed: 15355597]
30. Vargas-Madrado E, Almagro JC, Lara-Ochoa F. Structural Repertoire in V<sub>H</sub>Pseudogenes of Immunoglobulins: Comparison with Human Germline Genes and Human Amino Acid Sequences. *J Mol Biol.* 1995; 246:74–81. [PubMed: 7853406]
31. Korneev SA, Park J-H, O'Shea M. Neuronal Expression of Neural Nitric Oxide Synthase (nNOS) Protein Is Suppressed by an Antisense RNA Transcribed from an NOS Pseudogene. *J Neurosci.* 1999; 19:7711–7720. [PubMed: 10479675]
32. Ioffe YJ, Chiappinelli KB, Mutch DG, Zigelboim I, Goodfellow PJ. Phosphatase and tensin homolog (PTEN) pseudogene expression in endometrial cancer: a conserved regulatory mechanism important in tumorigenesis? *Gynecol Oncol.* 2011
33. Poliseno L, Salmena L, Zhang J, Carver B, Haveman WJ, Pandolfi PP. A coding-independent function of gene and pseudogene mRNAs regulates tumour biology. *Nature.* 2010; 465:1033–1038. [PubMed: 20577206]
34. Cornelis G, Heidmann O, Bernard-Stoeklin S, Reynaud K, Veron G, Mulot B, et al. From the Cover: Ancestral capture of syncytin-Car1, a fusogenic endogenous retroviral envelope gene involved in placentation and conserved in Carnivora. *Proc Natl Acad Sci U S A.* 2012; 109:E432–E441. [PubMed: 22308384]



35. Hornung V, Ablasser A, Charrel-Dennis M, Bauernfeind F, Horvath G, Caffrey DR, et al. AIM2 recognizes cytosolic dsDNA and forms a caspase-1-activating inflammasome with ASC. *Nature*. 2009; 458:514–518. [PubMed: 19158675]
36. Srinivasula SM, Poyet JL, Razmara M, Datta P, Zhang Z, Alnemri ES. The PYRIN-CARD protein ASC is an activating adaptor for caspase-1. *J Biol Chem*. 2002; 277:21119–21122. [PubMed: 11967258]
37. Stehlik C, Lee SH, Dorfleutner A, Stassinopoulos A, Sagara J, Reed JC. Apoptosis-associated speck-like protein containing a caspase recruitment domain is a regulator of procaspase-1 activation. *J Immunol*. 2003; 171:6154–6163. [PubMed: 14634131]
38. Kaltschmidt B, Kaltschmidt C, Hofmann TG, Hehner SP, Droge W, Schmitz ML. The pro- or anti-apoptotic function of NF-kappaB is determined by the nature of the apoptotic stimulus. *Eur J Biochem*. 2000; 267:3828–3835. [PubMed: 10849002]
39. Reuther-Madrid JY, Kashatus D, Chen S, Li X, Westwick J, Davis RJ, et al. The p65/RelA subunit of NF-kappaB suppresses the sustained, antiapoptotic activity of Jun kinase induced by tumor necrosis factor. *Mol Cell Biol*. 2002; 22:8175–8183. [PubMed: 12417721]
40. Carswell E, Old L, Kassel R, Green S, Fiore N, Williamson B. An endotoxin-induced serum factor that causes necrosis of tumors. *Proc Natl Acad Sci U S A*. 1975; 72:3666–3670. [PubMed: 1103152]
41. Miura M, Friedlander RM, Yuan J. Tumor necrosis factor-induced apoptosis is mediated by a CrmA-sensitive cell death pathway. *Proceedings of the National Academy of Sciences*. 1995; 92:8318–8322.
42. Schilling D, Thomas K, Nixdorff K, Vogel SN, Fenton MJ. Toll-Like Receptor 4 and Toll-IL-1 Receptor Domain-Containing Adapter Protein (TIRAP)/Myeloid Differentiation Protein 88 Adapter-Like (Mal) Contribute to Maximal IL-6 Expression in Macrophages. *J Immunol*. 2002; 169:5874–5880. [PubMed: 12421970]
43. Mariathasan S, Weiss DS, Dixit VM, Monack DM. Innate immunity against *Francisella tularensis* is dependent on the ASC/caspase-1 axis. *J Exp Med*. 2005; 202:1043–1049. [PubMed: 16230474]
44. Jones CL, Weiss DS. TLR2 signaling contributes to rapid inflammasome activation during *F. novicida* infection. *PLoS ONE*. 2011; 6:e20609. [PubMed: 21698237]
45. Sivak LE, Pont-Kingdon G, Le K, Mayr G, Tai K-F, Stevens BT, et al. A Novel Intron Element Operates Posttranscriptionally To Regulate Human N-myc Expression. *Mol Cell Biol*. 1999; 19:155–163. [PubMed: 9858540]
46. Tieri P, Termanini A, Bellavista E, Salvioli S, Capri M, Franceschi C. Charting the NF-kappaB pathway interactome map. *PLoS ONE*. 2012; 7:e32678. [PubMed: 22403694]
47. Kersse K, Verspurten J, Berghe TV, Vandenabeele P. The death-fold superfamily of homotypic interaction motifs. *Trends Biochem Sci*. 2011; 36:541–552. [PubMed: 21798745]
48. Kersse K, Vanden Berghe T, Lamkanfi M, Vandenabeele P. A phylogenetic and functional overview of inflammatory caspases and caspase-1-related CARD-only proteins. *Biochem Soc Trans*. 2007; 35:1508–1511. [PubMed: 18031255]
49. Porter KA, Kelley LN, George A, Harton JA, Dues KM. Class II transactivator (CIITA) enhances cytoplasmic processing of HIV-1 Pr55Gag. *PLoS ONE*. 2010; 5:e11304. [PubMed: 20585587]
50. Muse SV, Gaut BS. A likelihood approach for comparing synonymous and nonsynonymous nucleotide substitution rates, with application to the chloroplast genome. *Mol Biol Evol*. 1994; 11:715–724. [PubMed: 7968485]
51. Tamura K, Nei M. Estimation of the number of nucleotide substitutions in the control region of mitochondrial DNA in humans and chimpanzees. *Mol Biol Evol*. 1993; 10:512–526. [PubMed: 8336541]
52. Kosakovskiy SL, Frost SD. Not so different after all: a comparison of methods for detecting amino acid sites under selection. *Mol Biol Evol*. 2005; 22:1208–1222. [PubMed: 15703242]
53. Suzuki Y, Gojobori T. A method for detecting positive selection at single amino acid sites. *Mol Biol Evol*. 1999; 16:1315–1328. [PubMed: 10563013]
54. Pond SL, Frost SD, Muse SV. HyPhy: hypothesis testing using phylogenies. *Bioinformatics*. 2005; 21:676–679. [PubMed: 15509596]

55. Tamura K, Dudley J, Nei M, Kumar S. MEGA4: Molecular Evolutionary Genetics Analysis (MEGA) software version 4.0. *Mol Biol Evol.* 2007; 24:1596–1599. [PubMed: 17488738]
56. Wen X, Duus KM, Friedrich TD, de Noronha CM. The HIV1 protein Vpr acts to promote G2 cell cycle arrest by engaging a DDB1 and Cullin4A-containing ubiquitin ligase complex using VprBP/DCAF1 as an adaptor. *J Biol Chem.* 2007; 282:27046–27057. [PubMed: 17620334]
57. George TC, Fanning SL, Fitzgerald-Bocarsly P, Medeiros RB, Highfill S, Shimizu Y, et al. Quantitative measurement of nuclear translocation events using similarity analysis of multispectral cellular images obtained in flow. *J Immunol Methods.* 2006; 311:117–129. [PubMed: 16563425]

A.

M V S S A Q L D F N L Q A L L  
 GAGTCCACGTCAGACGAG **ATG** GTG TCT TCT GCA CAG CTG GAC TTC AAC CTG CAG GCT CTT CTG  
**G Q L S Q D D L C K F K S L I R T V S L G**  
 GGA CAG CTC AGC CAG GAT GAC TTG TGC AAG TTC AAG TC T CTG ATC AGG ACC GTC TCC CTG GGA  
**N E L Q K I P Q T**  
 AAT GAG CTG CAA AAG ATC CCC CAG ACA **TAG** GTAGACAAGGCTGATGGGAAGCAACTGGCAGAAATCA  
 TCACCAGCCATTGCCACAGCTACTGGATGAAGATAGAGACCATCCAGGCTTTTAAAAAGATGCACCGAGCGG  
 ATCTGTCTGAGAAAAGTAAAGGATGAACTCAGAGAAGACACTTTGAAATCAAGCCTGTATCATTAGGGAAAACA  
 GGGAAAGAAGAGCCAAAACCTATAGACCTGAAACAAATGCTGGGGCGTTTCGAAGCAGAAGCACTAGA  
gtttatagaaacggAGGAAGATGTCACCAGCCTAAGAGAAGctaaagaagtcttgaaggagaaaag  
 Exon1  
 Exon2  
 CCAGGTAAAGAGGATAGGTACAGGAGTATATTGAAGACGAAGTTCTGGCAAATGTGG AAAACCTGGCCTGGA  
 GACCTCAAAGTGGTCCATATTATGGCTCAGAGATACAAGATGCTGATCCCGTTCAGCAACCCAGGGTGCTTC  
 CCGGGCCCTGCCACACACGGTGGTGTGCTGCATGGTCTGCGGGCCTTGGGAAAACACGCTGGCCAAGAA

B.

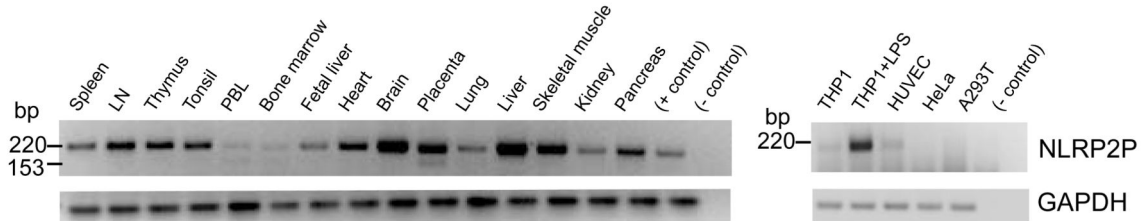


### Figure 1. NLRP2P sequence and mRNA expression

Partial genomic sequence from chromosome X and open reading frame of NLRP2P (A). Exons 1 and 2 are indicated (gray shading) and the start and stop codons of the open reading frame are shown (bold). The predicted protein sequence is indicated above in single letter code. Oligonucleotide primers used for PCR are underlined. The sequence targeted by NLRP2P/POP4 siRNA (small caps) is shown within the intron (lowercase). Expression of NLRP2P in human tissue and cell lines (B). The positive control is a mixture of human cDNAs supplied with the cDNA panels. Amplification without a specific template is also shown (negative control). LN = lymph node, PBL = peripheral blood leukocyte.

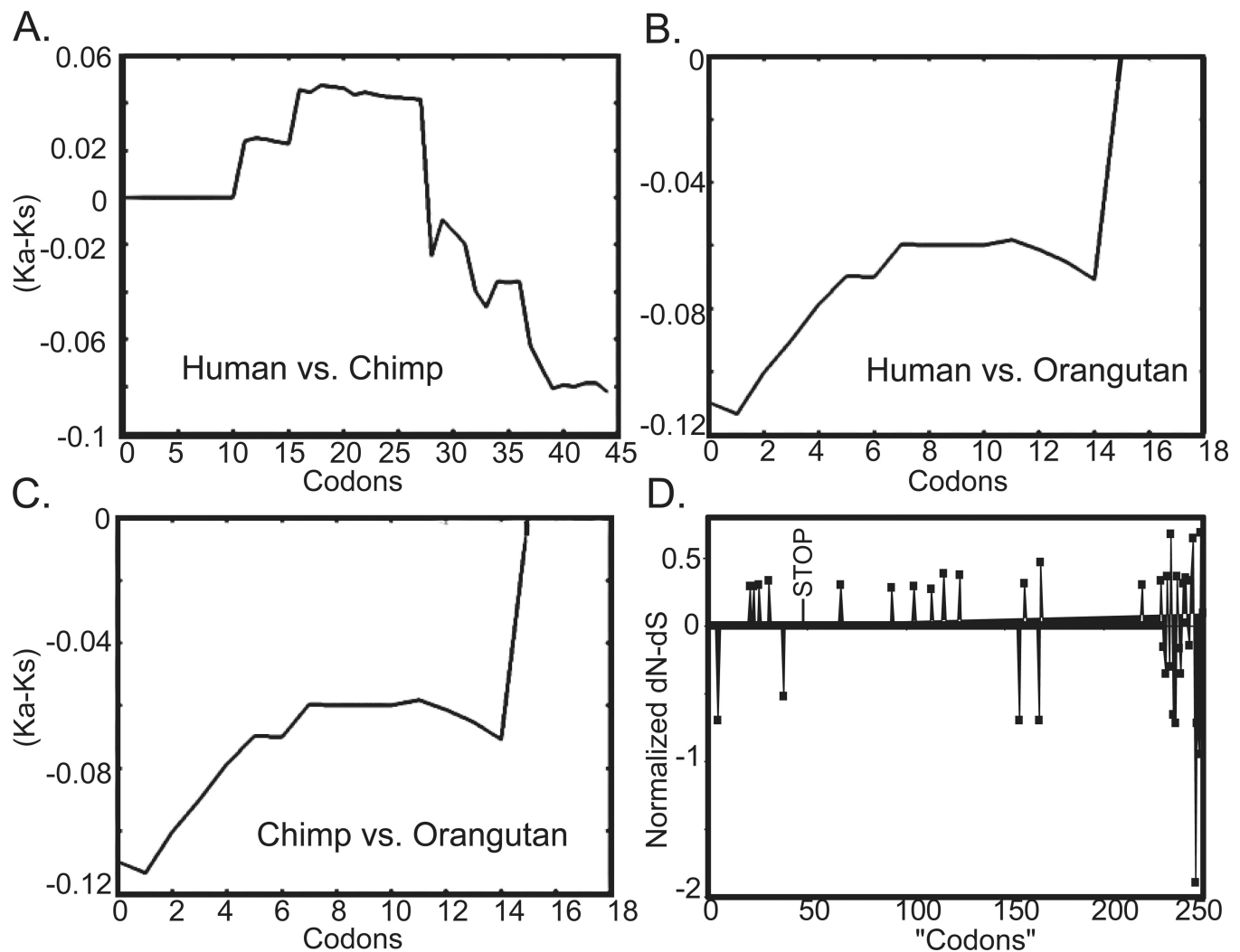


**Figure 2. The NLRP2P coding sequence is under purifying selection**

Sliding window analysis of Ka/Ks (SWAKK) results for (A) human NLRP2P (45 codons) versus chimp (45 codons), (B) human versus orangutan (20 codons), (C) chimp versus orangutan. Window size = 10. Values <1 indicate purifying selection. Codons with dN-dS >0 and <0 have p values >0.05 reflecting neutral selection. Maximum likelihood analysis of natural selection using codon-by-codon analysis for non-synonymous vs. synonymous mutations in the NLRP2P sequences (D). Codons with dN-dS=0 have p<0.0005 indicating purifying selection. Note: "Codons" beyond position 230 and 848 (1–250 shown) are not under selection (i.e. neutral).

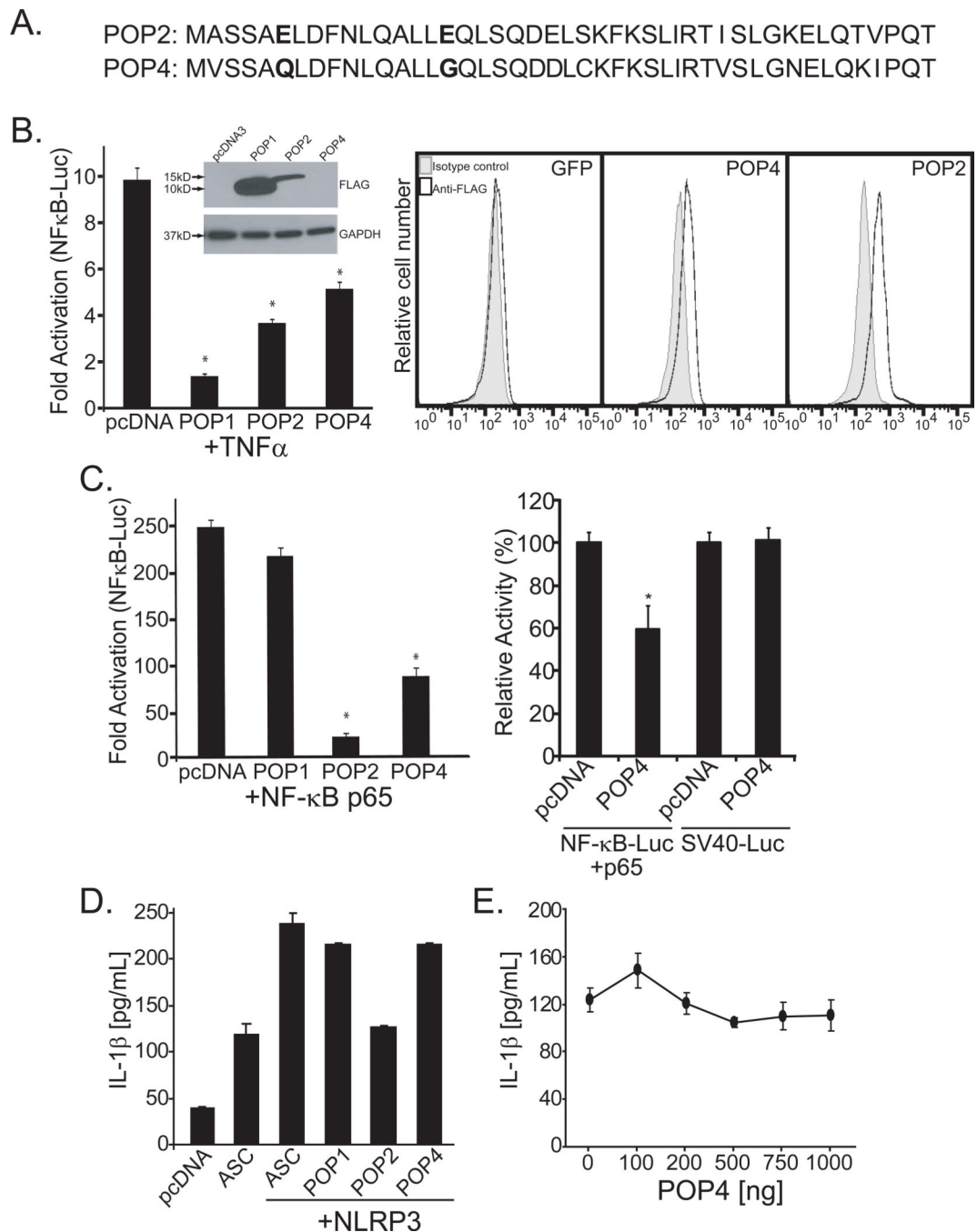


**Figure 3. POP4 impairs NF- $\kappa$ B activation but not inflammasome function**

Amino acid sequence of POP4 aligned with that of POP2 (A). Residues necessary for POP2-mediated inflammasome inhibition are shown in bold. POP mediated inhibition of NF- $\kappa$ B activation was measured by transfecting HEK-293 cells with 100 ng 3 $\times$ NF- $\kappa$ B luciferase and treating cells with TNF $\alpha$  (B, 10 ng/mL) or co-expressing p65 (C, left panel, 100ng) in the presence of 1  $\mu$ g indicated POP DNA. Immunoblot of transiently transfected HEK-293T cells showing expression of the FLAG-tagged POP proteins (B, inset). Immunofluorescent intracellular staining of transfected HEK-293T cells for FLAG-POP4 and FLAG-POP2

(control). POP4 (1  $\mu$ g) does not non-specifically decrease transcriptional activation mediated by the SV40 promoter of the pGL3-control reporter (C, right panel, 100ng). Inflammasome reconstitution assays were performed in HEK-293T cells and release of IL-1 $\beta$  elicited by the NLRP3 inflammasome (D) or ASC activation of caspase-1 (E) in the presence or absence of POP4 was measured by ELISA. \* $p$  < 0.01.

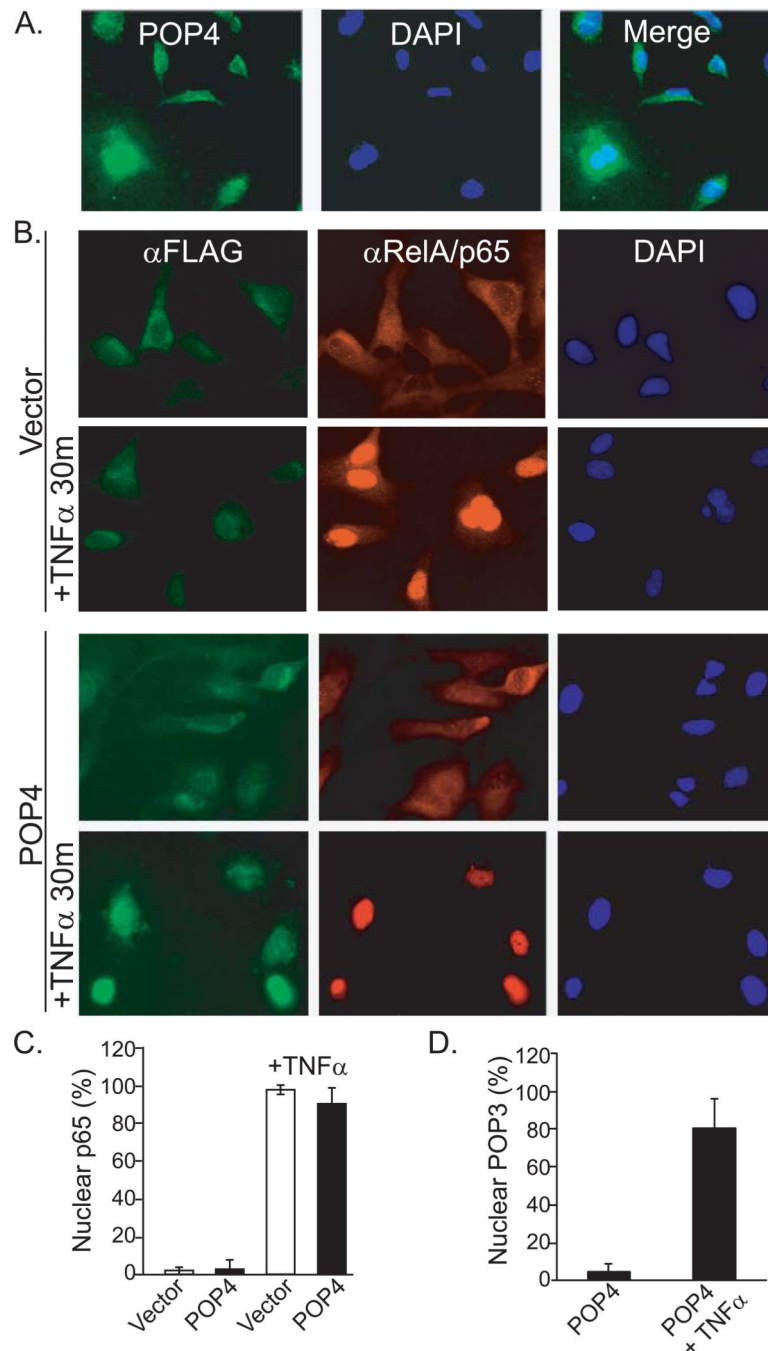


**Figure 4. POP4 localizes to the nucleus upon mitogen stimulation, but does not block p65 nuclear localization**

Localization of POP4 was determined by staining for FLAG-tag in HeLa cells transfected with FLAG-POP4 (1 $\mu$ g) and co-stained with DAPI (A). The impact of POP4 on p65 localization (B) was monitored in HeLa cells transfected with 1 $\mu$ g of empty vector or FLAG-POP4 and left untreated or stimulated for 30m with hTNF $\alpha$  (20ng/mL). Cells were stained with anti-FLAG and Alexa488 secondary antibody to detect FLAG-POP4 together with anti-p65 and Alexa594 secondary antibody plus DAPI. The percentage of POP4 expressing cells with nuclear p65 (C) or nuclear POP4 (D) in the absence or presence of

TNF $\alpha$  was determined from multiple images represented in (B). POP4 stable J774A.1 cells were produced by transfecting cells with FLAG-POP4. Expression was determined by flow cytometry for the intracellular FLAG tag from selected clones and a polyclonal population (D).



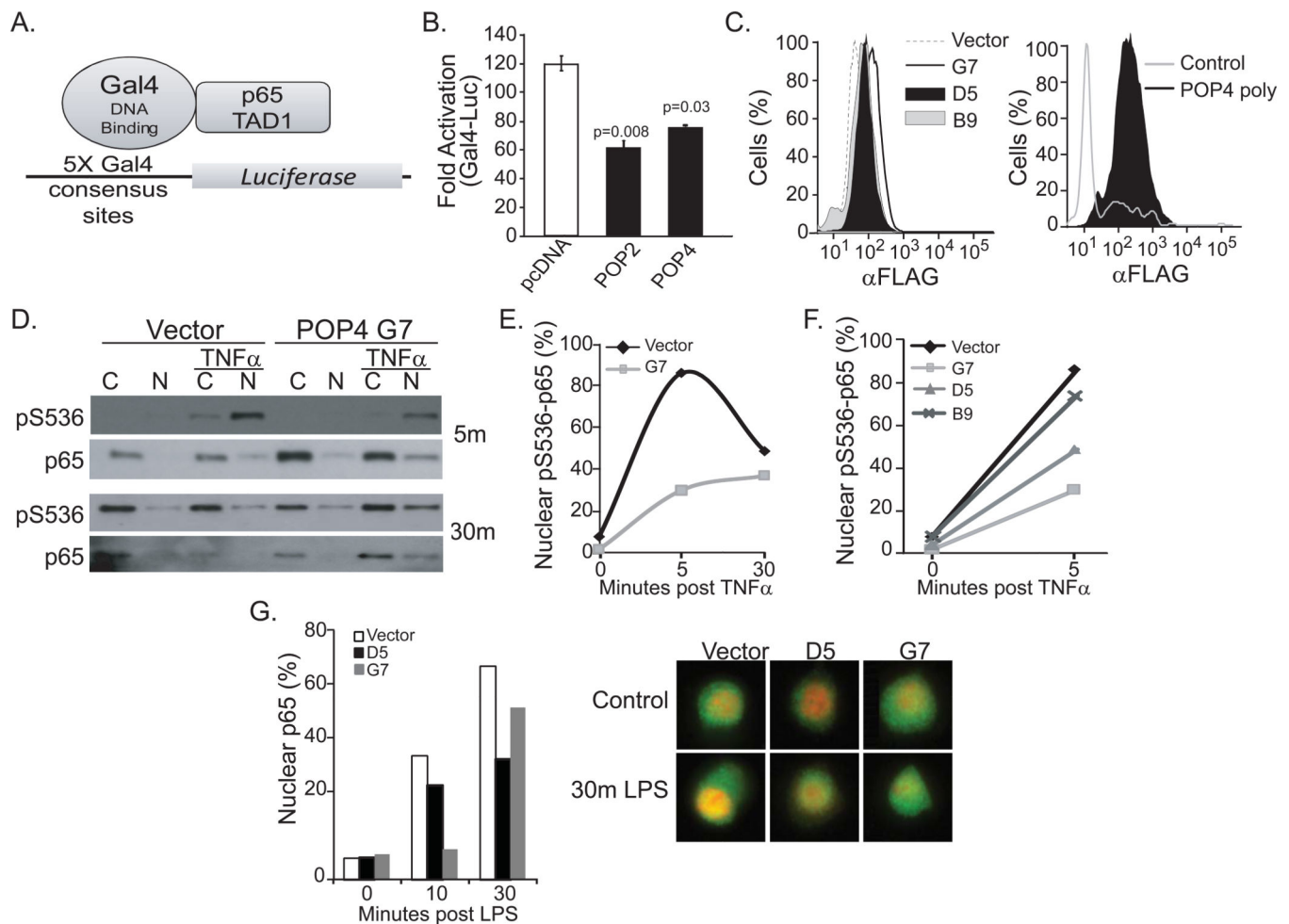


**Figure 5. POP4 blocks RelA/p65 transactivation by TAD1 by reducing S536 phosphorylation**  
 Model for the Gal4-p65 transactivation assay (A), TAD1 of RelA/p65 is comprised of residues 519–550. Gal4-p65TAD1-mediated transactivation of 5×Gal4-luciferase was monitored in HEK-293 cells in the presence of POP2 and POP4 (B). POP4 stable cells lines were produced by transfecting J774A.1 cells with FLAG-POP4 and clonal expression was determined by flow cytometry for intracellular FLAG (C). J774A.1 clones expressing either vector or POP4 were treated for 5m with TNFα (20 ng mL<sup>-1</sup>). Western blots for p65 and phosphorylated p65 (S536) and β-actin following cytoplasmic and nuclear fractionation (D). Bands were quantified by densitometric analysis and the relative percentage of nuclear, phosphorylated p65 (S536) versus total cellular p65 was calculated for the indicated clones and timepoints (E, F). J774A.1 POP4 and vector only clones were stimulated with LPS (200 ng/ml) and nuclear localization of p65 was assessed by measuring spectral similarity between cellular images obtained during flow cytometry (ImageStream). Relative frequencies of cells (out of >9000) with nuclear p65 are shown (G, left panel). Representative images of cells from the analysis exhibiting staining for DRAQ5 (nucleus, red), p65 (green), and co-localized nuclear p65/DRAQ5 (yellow) (G, right panel). For C–G, data are representative of at least two independent experiments.

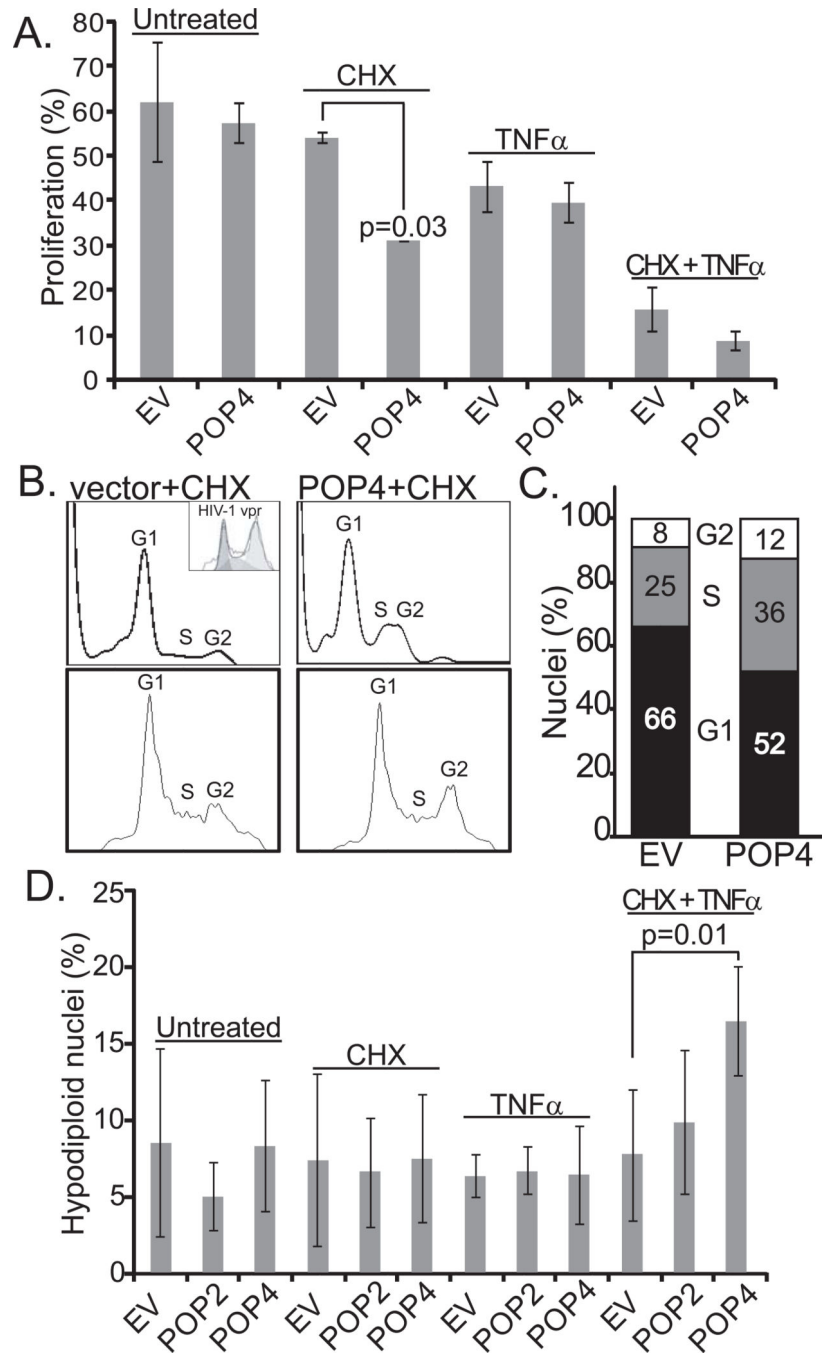


### Figure 6. POP4 alters cell cycle and enhances apoptosis

HeLa cells were transfected with either empty vector (EV) or POP4 and the next day treated with TNF $\alpha$  and/or cycloheximide as indicated for 24 h prior to enumeration and determination of cell proliferation (A). Cell cycle analysis following PI staining of cell nuclei from either EV or POP4 transfected cells left untreated or exposed to cycloheximide. HIV-1Vpr serves as a control for G2 arrest (B, two representative plots are shown). The percentage of cells in each stage of the cell cycle (C). Hypodiploid nuclei were gated and the percentage determined as an indicator of apoptotic cell death (D).

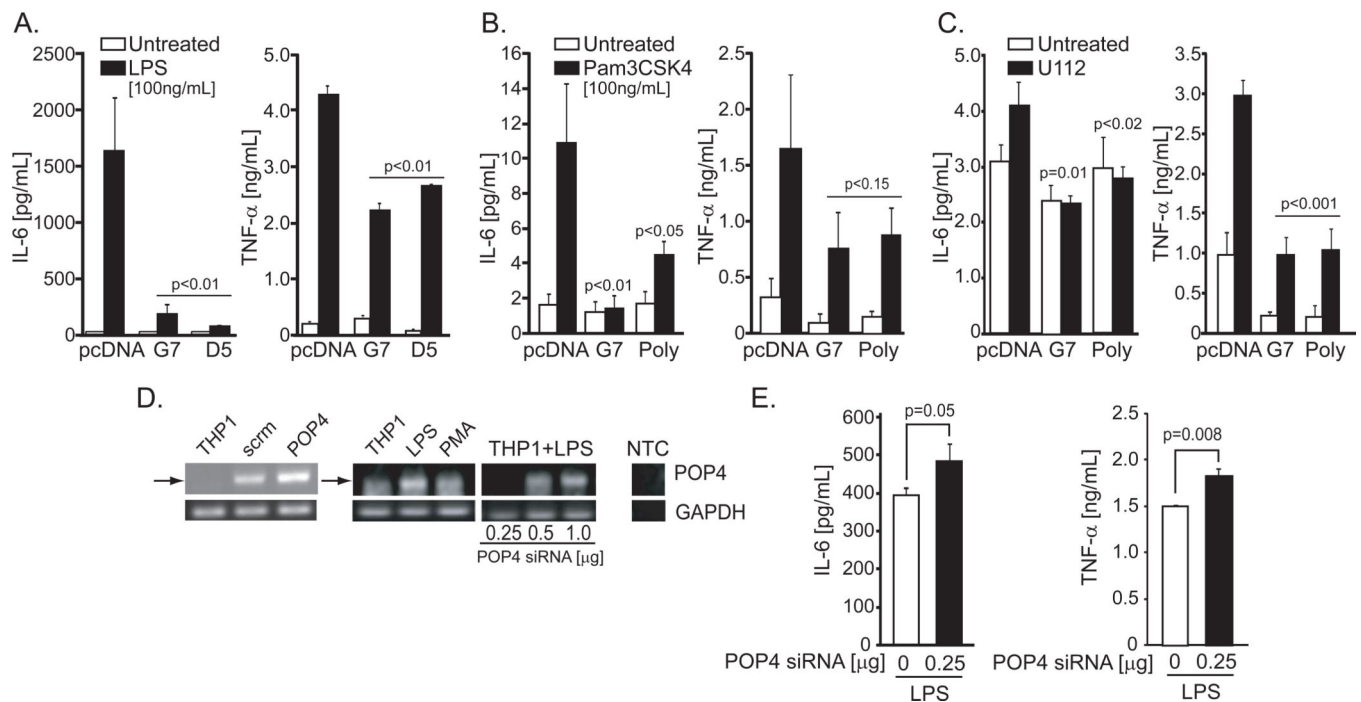


**Figure 7. POP4 reduces NF- $\kappa$ B-mediated cytokine release following stimulation with TLR ligands or infection**

J774 cells ( $2 \times 10^5$ ) were treated with either LPS (A) or Pam3CSK4 (B) or infected with *F. novicida* U112 (MOI=100, C) for 24 h and IL-6 and TNF $\alpha$  levels were measured by cytometric bead array. Control (scrambled, scrm) and POP4 siRNA induced POP4 expression in THP-1 cells (D, left panel). Effect of various doses of POP4 siRNA upon POP4 mRNA expression in PMA-differentiated THP-1 cells ( $2.5 \times 10^5$ ) treated post-PMA with or without LPS (200 ng/mL) for 6 h (D, right panels). Production of IL-6 and TNF $\alpha$  (E) for cells shown in (D). All data is the average of two or more independent experiments. Poly = pooled polyclonal populations of stable POP4-expressing J774A.1 transfectants.

**Table 1**

## Processed versus Non-Processed Pseudogenes

FEATURE	PSEUDOGENE TYPE <sup>1</sup>		
	PROCESSED	NON-PROCESSED	NLRP2P
Introns	N	Y	Y
Extra-locus	Y	N	Y
Genomic poly(A)	Y	N	Y
Flanked by direct repeats	Y	N	ND
Promoter	N	Y	Y
Expression	N	N	Y
Functional protein	N	N	?
Premature stop codon	Y	Y	Y
Alterations in splice sites	Y	Y	Y

<sup>1</sup> Characteristics of both pseudogene types are from those defined by D'Errico, *et al.*<sup>29</sup>

ND=not detected